Wireless Communication Technologies

Course No. 16:332:559 (Spring 2000)

Lecture 01-26-00

Lalitha Sankaranarayanan

lalitha@ustad.att.com

PATH LOSS IN MACROCELLS:

The theoretical model for path loss, L_p, for propagation close to the earth's surface was derived as:

$$L_p(dB) = 10\log\left[d/h_b h_m\right] \tag{1.1}$$

where h_m is the height of the mobile station (MS), h_b is the height of the base station (BS), d is the distance between the BS and the MS. This model does not obviously include the dependence of path loss on the propagation frequency and also does not include actual real environments with multiple paths resulting from reflections from a variety of sources.

Several highly useful empirical models for macrocellular systems have been obtained by curve fitting experimental data. Two of the more useful models for 900 MHz cellular systems are Hata's model based on Omura's prediction [1] method and Lee's model [2].

HATA'S MODEL:

Hata's empirical model is based on data collected in the city of Tokyo. This model can distinguish between man-made structures [3]. The path loss modeled here is for Japanese suburban areas and does not match North American suburban areas very well. Hata's model is expressed in terms of the following parameters:
carrier frequency: $150 \le f_c \le 1000$ (MHz)
BS antenna height: $30 \le h_b \le 200$ (m)
MS antenna height: $1 \le h_m \le 10$ (m)
and the distance between the BS and MS: $1 \le d \le 20$ (km)

The model is known to be accurate to within 1 dB for distances ranging from 1 to 20 km. With Hata's model, the path loss (in dB) is

$$L_p(dB) = \begin{cases} A + B\log_{10}(d) & \text{for urban area} \\ A + B\log_{10}[d] - C & \text{for suburban area} \\ A + B\log_{10}[d] - D & \text{for open area} \end{cases} \tag{1.2}$$

where

$$A = 69.55 + 26.16\log_{10}(f_c) - 13.82\log_{10}(h_b) - a(h_m)$$
$$B = 44.9 - 13.82\log_{10}(h_b)$$
$$C = 5.4 + 2[\log_{10}(f_c/28)]^2$$
$$D = 40.94 + 4.78[\log_{10}(f_c/28)]^2 - 18.33\log_{10}(f_c)$$

and

$$a(h_m) = \begin{cases} \left(1.1\log_{10}(f_c) - 0.7\right)h_m - \left(1.56\log_{10}(f_c) - 0.8\right) \\ \qquad\qquad\qquad\qquad \text{for medium or small city} \\ 8.28\left(\log_{10}(1.54h_m)\right)^2 - 1.1 \qquad \text{for } f_c \leq 200 \text{ MHz for large city} \\ 3.2\left(\log_{10}(11.75h_m)\right)^2 - 4.97 \quad \text{for } f_c \geq 400 \text{ MHz for large city} \end{cases}$$

LEE'S MODEL:

Lee's empirical path loss prediction model is also accurate and easy to use [2]. He method is generally used to predict the path loss over flat terrain. If the actual terrain is not flat, but for example hilly, there will be prediction errors. Two parameters are required for Lee's path loss prediction mode are:
the power at a 1 mile (1.6 km) point of interception $\mu_{\Omega_{d_0}}$

and the path loss exponent β.

The received signal power at a distance of d km from the transmitter can be expressed as

$$\mu_\Omega = 10\log_{10}\left(\mu_{\Omega_{d_0}}\left(\frac{d_0}{d}\right)^\beta\left(\frac{f_c}{f}\right)^n\alpha_0\right) \text{ dBm} \qquad (1.3)$$

where d is in kilometers and d_0 = 1.6 km. The parameter α_0 is a corrective factor used to account for different BS and MS antenna heights, transmit powers, and antenna gains. The following set of nominal conditions are assumed in Lee's path loss model:

- frequency f_c = 900 MHz
- BS antenna height = 30.48 m
- BS transmit power = 10 Watts
- BS antenna gain = 6 dB above dipole gain
- MS antenna height = 3 m
- MS antenna gain = 0 dB above dipole gain

If the actual conditions are different from those listed above, then we compute the following parameters to determine the correction factor α_0 to use.

$$\alpha_1 = \left(\frac{\text{new BS antenna height (m)}}{30.48\text{m}} \right)^2$$
$$\alpha_2 = \left(\frac{\text{new MS antenna height (m)}}{3\text{m}} \right)^{\xi}$$
$$\alpha_3 = \left(\frac{\text{new transmitter power}}{10\text{W}} \right)^2 \qquad (1.4)$$
$$\alpha_4 = \frac{\text{new BS antenna gain}}{4}$$
$$\alpha_4 = \text{different antenna gain correction factor at the MS}$$

From these parameters, the correction factor α_0 is:

$$\alpha_0 = \alpha_1 \cdot \alpha_2 \cdot \alpha_3 \cdot \alpha_4 \cdot \alpha_5 \qquad (1.5)$$

The parameters $\mu_{\Omega_{d_0}}$ and β have been found from empirical measurements, and are listed in Table 1 below.

Terrain	$\mu_{\Omega_{d_0}}$ (dBm)	β
Free Space	-45	2
Open Area	-49	4.35
North American Suburb	-61.7	3.84
North American Urban (Philadelphia)	-70	3.68
North American Urban (Newark)	-64	4.31
Japanese Urban (Tokyo)	-84	3.05

Table 1 Parameters for Lee's path loss prediction model in various propagation environments

The value of *n* in equation (1.3) ranges between 2 and 3 with the exact value depending upon the carrier frequency and the geographical area. For $f_c \leq 450$ MHz in a suburban or open area, $n = 2$ is recommended. In an urban area with $f_c > 450$ MHz, $n = 3$ is recommended. The value of in (1.4) is also determined from empirical data

$$\xi = \begin{cases} 2 & \text{for a MS antenna height} > 10 \text{ m} \\ 3 & \text{for a MS antenna height} < 3 \text{ m} \end{cases} \qquad (1.6)$$

The path loss L_p is simply the difference between the transmitted and power field strengths in dB, $L_p = \Omega_p - \mu_{\Omega_{d_0}}$. By using the above parameters for $\mu_{\Omega_{d_0}}$, the following path losses (in dB) can be obtained

$$L_p = \begin{cases} 80.92 + 20.0\log_{10}(d) + 10n\log_{10}(f/900) - \alpha_0 & \text{Free Space} \\ 80.11 + 43.5\log10(d) + 10n\log_{10}(f/900) - \alpha_0 & \text{Open Area} \\ 93.86 + 38.4\log10(d) + 10n\log_{10}(f/900) - \alpha_0 & \text{Suburban} \\ 102.59 + 36.8\log10(d) + \log_{10}(f/900) - \alpha_0 & \text{Philadelphia} \\ 95.2 + 43.1\log10(d) + \log_{10}(f/900) - \alpha_0 & \text{Newark} \\ 117.37 + 30.5\log10(d) + \log_{10}(f/900) - \alpha_0 & \text{Tokyo} \end{cases} \quad (1.7)$$

These typical models from Lee's model are plotted in Figure 3 and the values from Hata's model (large city) are plotted in Figure 4, for a BS height of 70 m, a MS antenna height of 1.5 m, and a carrier frequency of 900 MHz.

PATH LOSS IN OUTDOOR MICROCELLS

Most of the future PCS microcellular systems are expected to operate in 1800-2000 MHz frequency bands. Some studies have suggested that path losses experienced at 1845 MHz are about 10 dB larger than those experienced at 955 MHz when all other parameters are kept constant [4]. The COST231 study has resulted in two models for urban microcellular propagation, the COST231-Hata model and the COST231-Walfish-Ikegami model.

COST231-HATA MODEL

The COST231-Hata model extends the Hata's model for use in the 1500-2000 MHz frequency range where it is known that Hata's model under estimates the path loss. The COST231-Hata model is expressed in terms of the carrier frequency $1500 \le f_c \le 2000$ (MHz), BS antenna height $30 \le h_b \le 200$ (m), MS antenna height $1 \le h_m \le 10$ (m), and distance $1 \le d \le 20$ (km). In particular, the path loss (in dB) with the COST231-Hata model is:

$$L_p = A + B\log_{10}(d) + C \quad (1.8)$$

where

$$A = 46.3 + 33.9\log_{10}(f_c) - 13.28\log_{10}(h_b) - a(h_m)$$
$$B = 44.9 - 6.55\log_{10}(h_b)$$
$$C = \begin{cases} 0 & \text{for medium city and suburban areas} \\ & \text{with moderate tree density} \\ 3 & \text{for metropolitan areas} \end{cases}$$

Although the Hata and the COST231Hata models are limited to BS antenna heights greater than 30 m, they can be used for lower BS antenna heights provided the surrounding buildings are well below the BS antenna heights. They should not be used to predict path loss in urban canyons. The COST231-Hata model is good down to a path length of 1 km. It should not be used for smaller ranges, where path losses become highly dependent on local topography.

COST231-WALFISH-IKEGAMI MODEL

The COST231-Walfish-Ikegami model is applicable to cases where the BS antennas are either above or below the rooftops. However, the model is not very accurate when the BS antennas are about the same height as the rooftops. For LOS propagation in a street canyon, the path loss (in dB) is

$$L_p = 42.6 + 26\log_{10}(d) + 20\log_{10}(f_c), \quad d \geq 20\ m \tag{1.9}$$

where the first constant is chosen so that L_p is equal to the free-space path loss at a distance of 20 m. The model parameters are the distance d (in kms) and the carrier frequency f_c (MHz). As shown in Figure 1 below, the path loss for non line-of-sight (NLOS) propagation is expressed in terms of the building heights, h_{Roof}, street widths, w, building separation, b, and road orientation with respect to the direct radio path, ϕ. The path loss components is composed of three terms, namely,

$$L_p = \begin{cases} L_0 + L_{rts} + L_{msd} & \text{for } L_{rts} + L_{msd} \geq 0 \\ L_0 & \text{for } L_{rts} + L_{msd} < 0 \end{cases} \tag{1.10}$$

where L_0 is the free space propagation loss, L_{rts} is the roof-to-street diffraction and scatter loss, and L_{msd} is the multi-screen diffraction loss. The free-space loss is

$$L_0 = 32.4 + 20\log_{10}(d) + 20\log_{10}(f_c) \tag{1.11}$$

The roof-top-to-street diffraction and scatter loss is

$$L_{rts} = -16.9 - 10\log_{10}(w) + 10\log_{10}(f_c) + 20\log_{10}\Delta h_m + L_{ori} \tag{1.12}$$

where

$$L_{ori} = \begin{cases} -10 + 0.354(\phi), & 0 \leq \phi \leq 35^\circ \\ 2.5 + 0.075(\phi - 35) & 35 \leq \phi \leq 55^\circ \\ 4.0 - 0.114(\phi - 55) & 55 \leq \phi \leq 90^\circ \end{cases} \tag{1.13}$$

and

$$\Delta h_m = h_{Roof} - h_m \tag{1.14}$$

The multi-screen diffraction loss is

$$L_{msd} = L_{bsh} + k_a + k_d \log_{10}(d) + k_f \log_{10}(f_c) - 9\log_{10}(b) \tag{1.15}$$

where

$$L_{bsh} = \begin{cases} -18\log_{10}(1 + \Delta h_b) & h_b \geq h_{Roof} \\ 0 & h_b \leq h_{Roof} \end{cases} \tag{1.16}$$

$$k_a = \begin{cases} 54, & h_b > h_{Roof} \\ 54 - 0.8h_b, & d \geq 0.5\text{km and } h_b \leq h_{Roof} \\ 54 - 0.8\Delta h_b d/0.5 & d < 0.5\text{km and } h_b \leq h_{Roof} \end{cases} \tag{1.17}$$

$$k_d = \begin{cases} 18, & h_b > h_{Roof} \\ 18 - 15\Delta h_b / h_{Roof}, & h_b \leq h_{Roof} \end{cases}$$

$$k_f = -4 + \begin{cases} .7(f_c/925 - 1), & \text{medium city and suburban} \\ 1.5(f_c/925 - 1), & \text{metropolitan area} \end{cases} \tag{1.18}$$

and

$$\Delta h_b = h_b - h_{Roof} \tag{1.19}$$

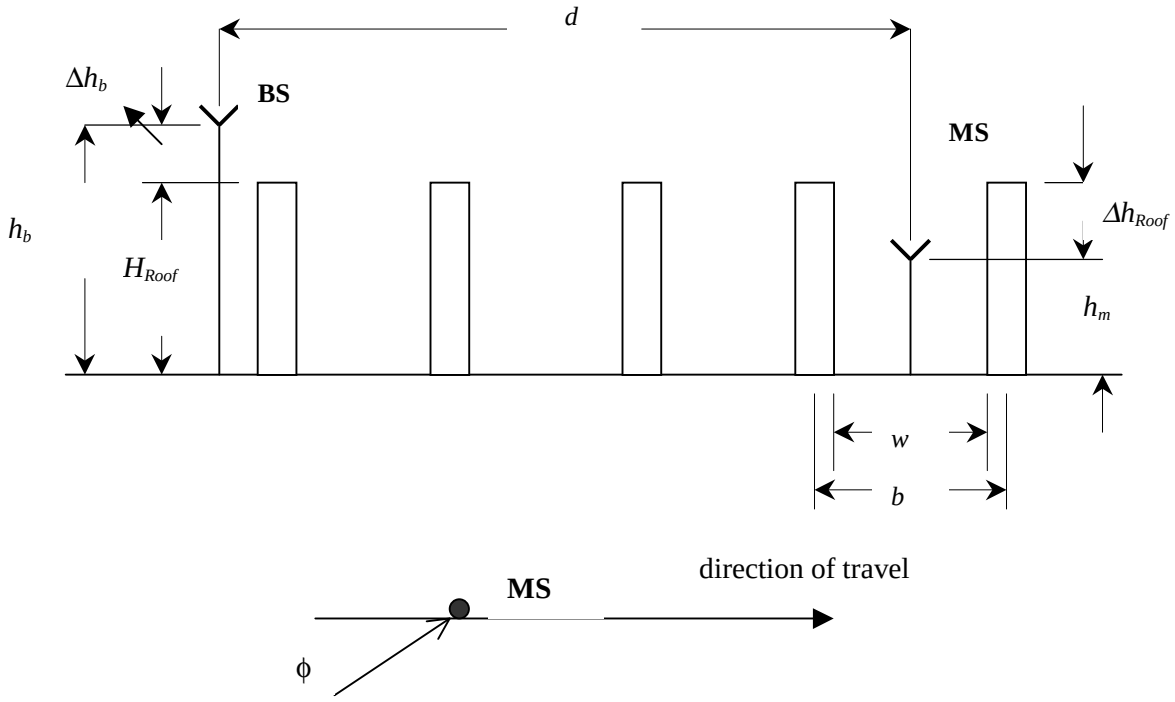

Figure 1 Definition of parameters used in COST231-Walfish-Ikegami model

The term k_a is the increase in path loss for BS antennas below the rooftops of adjacent buildings. The terms k_d and k_f control the dependency of the multi-screen diffraction loss on the distance and frequency, respectively. The model is valid for the following ranges of parameters, $800 \le f_c \le 2000$ (MHz), $4 \le h_b \le 50$ (m), $1 \le h_m \le 3$ MHz, and $0.02 \le d \le 5$ (km). If no data on the structure of the buildings and roads are available, the following default values are recommended, $b = 20 \ldots 50$ (m), $w = b/2$, $\phi = 90°$, and h_{Roof} = 3×number of floors+roof (m), where roof = 3 (m) (pitched) and 0 (m) flat. The COST231-Walfish-Ikegami model works best for $h_b >> h_{\text{Roof}}$. Large errors can be expected for $h_b \approx h_{\text{Roof}}$. The model is poor for $h_b << h_{\text{Roof}}$ because the terms in (1.17) do not consider wave guiding in street canyons and diffraction at street corners.

PATH LOSS IN STREET MICROCELLS

For ranges less than 500 m and antenna heights less than 20 m, some empirical measurements have shown that the received signal strength for LOS propagation along city streets can be accurately described by the two-slope model [5], [6].

$$\mu_\Omega = 10\log_{10}\left(\frac{A}{d^a\left(1+d/g\right)^b}\right) \quad \text{dBm} \tag{1.20}$$

where A is a constant and d (m) is the distance. Close into the BS, free space propagation will prevail so that a = 2. The parameter g is called the breakpoint and ranges from 150 to 300 m. At large distances, an inverse-fourth to -eight power law is experienced so that b ranges from 2 to 6. The parameters a and b reflect path loss with values ranging from free space propagation values of 2 to higher. The breakpoint g occurs when the Fresnel zone between the two antennas just touches the ground assuming a flat surface. This distance is

$$g = \frac{1}{\lambda_c}\sqrt{\left(\Sigma^2-\Delta^2\right)-2\left(\Sigma^2+\Delta^2\right)\left(\frac{\lambda_c}{2}\right)^2+\left(\frac{\lambda_c}{2}\right)^4} \tag{1.21}$$

where $\Sigma = h_b + h_m$ and $\Delta = h_b - h_m$. For high frequencies this distance can be approximated as $g = 4h_bh_m/\lambda$. Note that the breakpoint is dependent on the frequency, with the breakpoint at 1.8 GHz being about twice that at 900 MHz. The model parameters that were obtained by Harley are shown in Table 2.

Street microcells may also exhibit NLOS propagation when a MS rounds a street corner as shown in Figure 2 below. In this case, the average received signal can drop by 25-30 dB over distances as small as 10 m for low antenna heights in an area with multi-story buildings. A loss in signal strength of 25-30 dB can occur over distances of 40-50 m for low antenna heights in a region of only one- or two-story buildings.

Grimlund and Gudmundson have proposed an empirical street corner path loss model. Their model assumes LOS propagation until the MS reaches the street corner. The NLOS propagation after rounding the street corner is modeled by assuming LOS propagation from an imaginary transmitter that is located at the street corner having a transmit power equal to the received power at the street corner from the serving BS. Then the received signal strength in dBm is given by:

$$\mu_\Omega = \begin{cases} 10\log_{10}\left(\dfrac{A}{d^a\left(1+d/g\right)^b}\right) & d \le d_c \\ 10\log_{10}\left(\dfrac{A}{d^a\left(1+d/g\right)^b}\cdot\dfrac{1}{\left(d-d_c\right)^a\left(1+\left(d-d_c\right)/g\right)^b}\right) & d > d_c \end{cases} \tag{1.22}$$

where d_c (m) is the distance between the serving BS and the corner.

Base Antenna Height (m)	a	b	Break point g (m)
5	2.30	-0.28	148.6
9	1.48	0.54	151.8
15	0.40	2.10	143.9
19	-0.96	4.72	158.3

Table 2 Two-slope path loss parameters obtained by Harley [5]

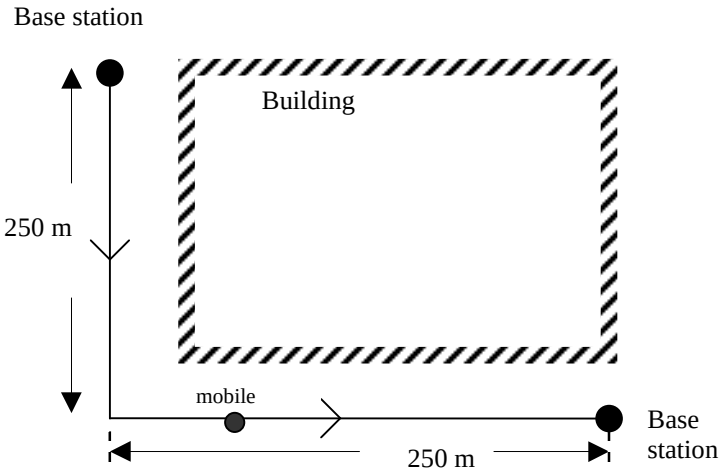

Figure 2 The corner effect in a street microcell environment

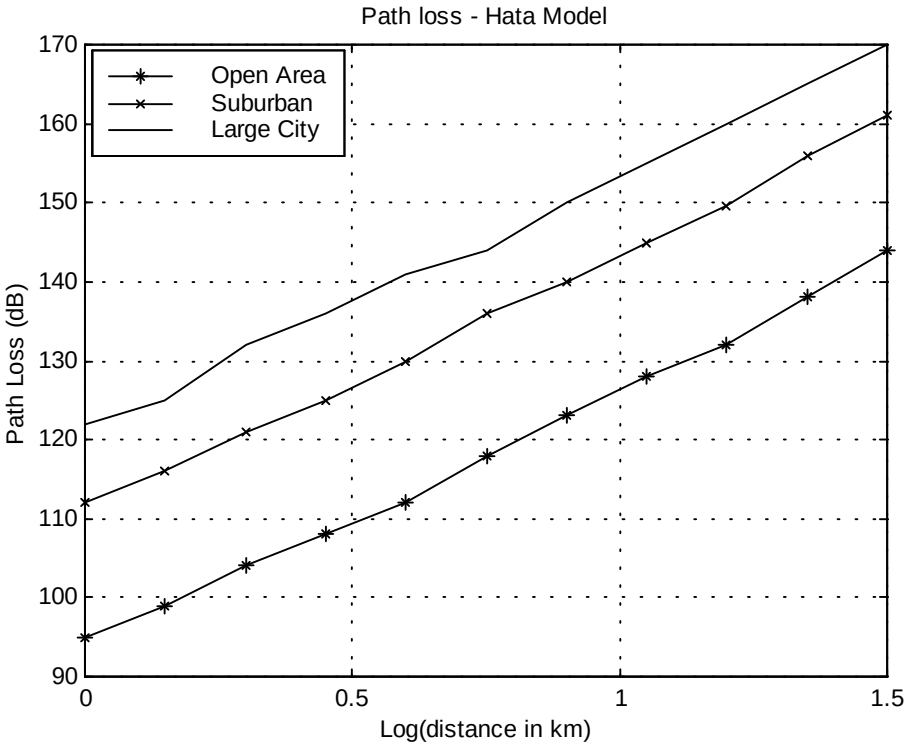

Figure 3 Path loss obtained from Lee's model

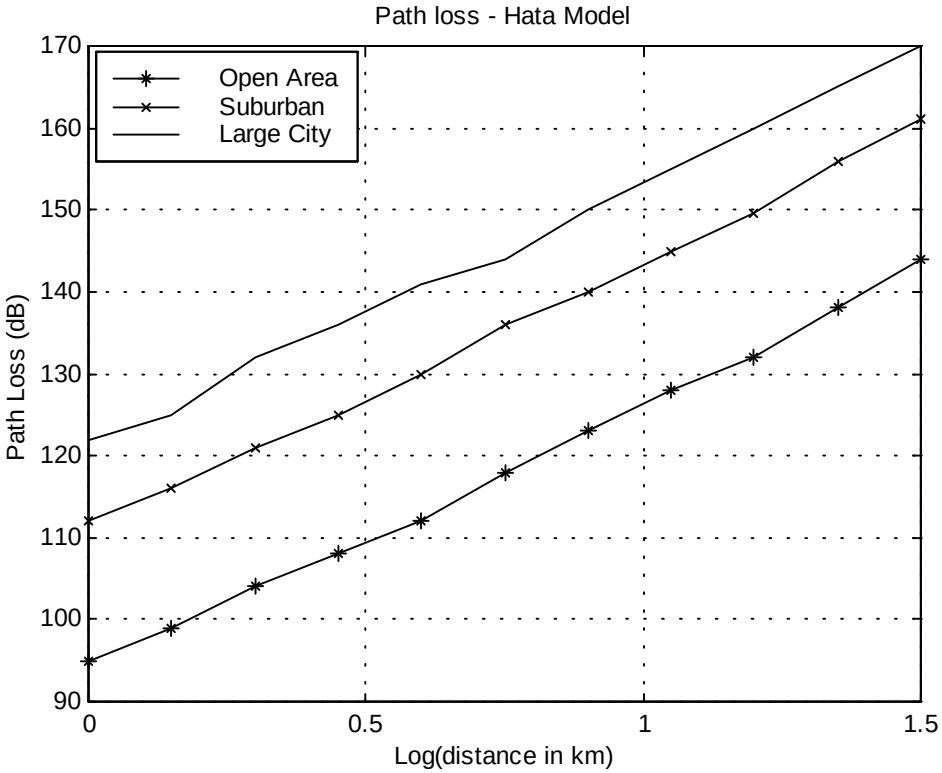

Figure 4 Path loss obtained by using Hata's model

Wireless Communication Technologies

Course No. 16:332:559 (Spring 2000)

Lecture 01-31-00

Lalitha Sankaranarayanan

lalitha@ustad.att.com

SMALL SCALE FADING AND MULTIPATH:

Small-scale fading, or simply fading, is used to describe the rapid fluctuation of the amplitude of a radio signal over a short period of time or travel distance, so that large-scale path loss effects (derived in the previous lecture) may be ignored. Fading is caused by the interference of two of more versions of the transmitted signal which arrive at the receiver at slightly different times. These waves, called *multipath* waves, combine at the receiver antenna to give a resultant signal which can vary widely in amplitude and phase, depending on the distribution of the intensity and relative propagation time of the waves and the bandwidth of the transmitted signal.

A typical cellular radio system consists of a collection of base stations (BSs) that are relatively free from local scatterers. In a macrocellular environment, the BS antennas are well elevated above the local terrain. No direct line-of-sight (LOS) path exists between the BS and the MS antennas, because of natural and man-made objects that are in the immediate vicinity of the MS. As a consequence of reflections, scattering, and diffraction, multiple place waves arrive at a MS from many different directions and with different delays as shown in Figure 5. This property is called multipath propagation.

Multipath in the radio channel creates small-scale fading effects. The three most important effects are:

- Rapid changes in signal strength over a small travel distance or time interval.
- Random frequency modulation due to varying Doppler shifts on different multipath signals.
- Time dispersion (echoes) caused by multipath propagation delays, resulting in inter-symbol interference.

Factors Influencing Small-Scale Fading:

Many physical factors in the radio propagation channel influence small-scale fading. These include the following [7]:

- Multipath propagation — The presence of reflecting objects and scatterers in the channel creates a constantly changing environment that dissipates the signal energy in amplitude, phase, and time. The random phase and amplitudes of the different multipath components cause fluctuations in signal strength, thereby inducing small-scale fading, signal distortion, or both.
- Speed of the mobile — The relative motion between the BS and the MS results in random frequency modulation due to different Doppler shifts on each of the multipath components. Doppler shift will be positive or negative depending on the direction of motion of the MS relative to the BS.
- Speed of surrounding objects — If objects in the radio channel are in motion, they induce a time varying Doppler shift on multipath components. If the surrounding objects move at a greater rate than the mobile, then this effect dominates the small-scale fading. Otherwise, motion of the surrounding objects can be ignored.

- The bandwidth of the transmitted signal — If the transmitted signal bandwidth is greater than the "bandwidth" of the multipath channel, then the received signal will be distorted, but the received signal will not fade much over the local area (i.e., the small-scale fading will not significant). Channel transmission bandwidth can be characterized by the *coherence bandwidth*, which is related to the specific multipath structure of the channel. The coherence bandwidth is the measure of the maximum frequency difference for which signals are still strongly correlated in amplitude. If the transmitted signal has a narrow bandwidth as compared to the channel, the amplitude of the signal will change rapidly, but the signal will not be distorted in time.

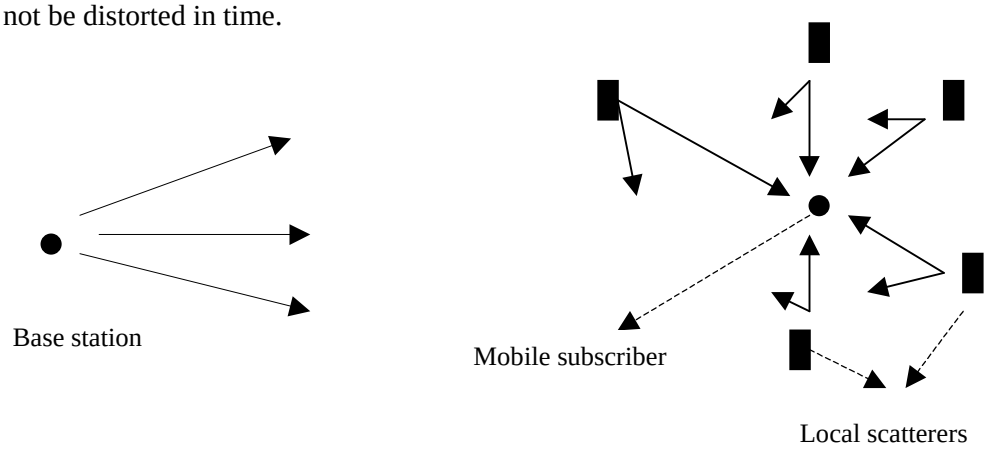

Figure 5 Typical macrocellular environment

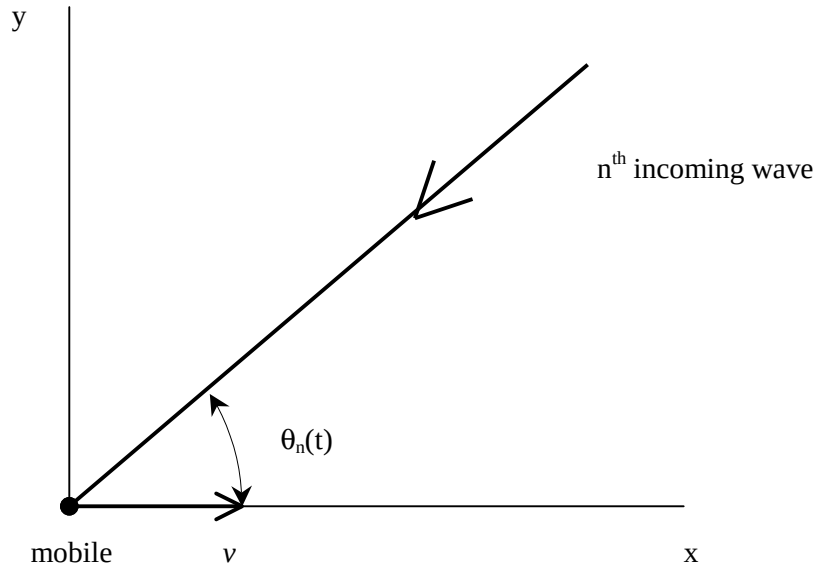

Figure 6 A typical plane wave component incident on a MS receiver

FREQUENCY-NON-SELECTIVE (FLAT) MULTIPATH FADING

Figure 6 depicts a horizontal *x-y* plane with a MS moving along the x-axis with velocity *v*. In portable and mobile radio applications the transmitted signals are usually vertically polarized and, therefore, the electric field is aligned with the *z*-axis. The n^{th} plane wave arrives at the MS

antenna with an angle of incidence $\theta_n(t)$. The MS movement introduces a Doppler, or frequency, shift into the incident plane wave, given by

$$f_{D,n}(t) = f_m \cos\theta_n(t) \quad \text{Hz} \tag{2.1}$$

where $f_m = v/\lambda_c$ and λ_c is the wavelength of the arriving place wave. Plane waves arriving from the direction of motion will experience a positive Doppler shift, while those arriving opposite from the direction of the motion will experience a negative Doppler shift.

Consider the transmission of the band-pass signal

$$s(t) = \mathrm{Re}\left\{u(t)e^{j2\pi f_c t}\right\} \tag{2.2}$$

where $u(t)$ is the complex low-pass signal, f_m is the carrier frequency, and Re{z} denotes the real part of z. If the channel is comprised of N paths, then the received band-pass waveform is

$$x(t) = \mathrm{Re}\left\{r(t)e^{j2\pi f_c t}\right\} \tag{2.3}$$

where the received complex low-pass signal r(t) is given by

$$r(t) = \sum_{n=1}^{N} \alpha_n(t) e^{-j2\pi\left[(f_c + f_{D,n}(t))\tau_n(t) - f_{D,n}(t)t\right]} u(t - \tau_n(t)) \tag{2.4}$$

and $\alpha_n(t)$ and $\tau_n(t)$ are the amplitude and time delay, respectively, associated with the nth path. The received complex low-pass signal can be rewritten as

$$r(t) = \sum_{n=1}^{N} \alpha_n(t) e^{-j\phi_n(t)} u(t - \tau_n(t)) \tag{2.5}$$

where

$$\phi_n(t) = 2\pi\left\{(f_c + f_{D,n}(t))\tau_n(t) - f_{D,n}(t)t\right\} \tag{2.6}$$

is the phase associated with the nth path. From (2.5), the channel can be modeled by a time-variant linear filter having the complex low-pass impulse response

$$c(t,\tau) = \sum_{n=1}^{N} \alpha_n(t) e^{-j\phi_n(t)} \delta(\tau - \tau_n(t)) \tag{2.7}$$

where $c(\tau,t)$ is the channel response at time t to an impulse response applied at time $t - \tau$ and $\delta(\cdot)$ is the dirac delta function.

From (2.5) and (2.6), several interesting observations can be made. Since $f_c + f_{D,,n}(t)$ is very large, a small change in the path delay $\tau_n(t)$ causes a large change in the phase $\phi_n(t)$. At any time t these random phase may result in the constructive or destructive interference of the components. The amplitudes $\alpha_n(t)$ depend on the cross sectional area of the nth scatterer or the length of the nth diffracting surface. However, these quantities do not change significantly over small spatial distances. Therefore, fading is primarily due to time variations $\phi_n(t)$ in the random phases that are caused by the Doppler shifts $f_{D,,n}(t)$.

Sometimes the channel is characterized by either a direct LOS path or a specular component from a strong (fixed) local scatterer. In this case, the amplitude $\alpha_0(t)$ is significantly larger than the other $\alpha_n(t)$. These special cases are characterized in the following sections with simplifications for these cases resulting in closed form solutions for the received signal correlation and power spectral density.

RECEIVED SIGNAL CORRELATION AND POWER SPECTRAL DENSITY

It is apparent that the different frequency components in a signal will be affected differently by the multipath-fading channel. However, for narrow-band signals where the signal bandwidth is very small compared to the carrier frequency, it suffices to derive the characteristics of the received complex low-pass signal by considering the transmission of an unmodulated carrier. For an unmodulated carrier, the received complex low-pass signal is

$$r(t) = \sum_{n=1}^{N} \alpha_n(t) e^{-j\phi_n(t)} \tag{2.8}$$

Using (2.3), the received band-pass signal can be expressed in the quadrature form

$$x(t) = r_I(t)\cos 2\pi f_c t - r_Q(t)\sin 2\pi f_c t \tag{2.9}$$

where

$$r_I(t) = \sum_{n=1}^{N} \alpha_n(t)\cos(\phi_n(t)) \tag{2.10}$$

$$r_I(t) = \sum_{n=1}^{N} \alpha_n(t)\sin(\phi_n(t)) \tag{2.11}$$

and $r(t) = r_I(t) + jr_Q(t)$. For large N, the central limit theorem can be invoked so that the quadrature components $r_I(t)$ and $r_Q(t)$ can be treated as independent Gaussian random processes. Assuming that the random processes are wide sense stationary (i.e., $f_{D,n}(t) = f_{D,n}$, $\alpha_n(t) = \alpha_n$, and $\tau_n(t) = \tau_{D,n}$), and assuming that $x(t)$ is wide sense stationary, the autocorrelation of $x(t)$ is

$$\begin{aligned}\phi_{xx}(t) &= E\left[x(t)x(t+\tau)\right] \\ &= E\left[r_I(t)r_I(t+\tau)\right]\cos 2\pi f_c\tau - E\left[r_Q(t)r_Q(t+\tau)\right]\sin 2\pi f_c\tau \\ &= \phi_{r_I r_I}(t)\cos 2\pi f_c\tau - \phi_{r_Q r_Q}(t)\sin 2\pi f_c\tau\end{aligned} \tag{2.12}$$

Note that

$$\phi_{r_I r_I}(\tau) = \phi_{r_Q r_Q}(\tau) \tag{2.13}$$

$$\phi_{r_I r_Q}(\tau) = -\phi_{r_Q r_I}(\tau) \tag{2.14}$$

It is reasonable to assume that the phases $\phi_n(t)$ and $\phi_m(t)$ are independent for n ≠ m since their associated delays and Doppler shifts are independent. Furthermore, the phases $\phi_n(t)$ can be assumed to be uniformly distributed over [-π, π], since $f_c\tau_n(t) >> 1$. By using these properties, it is straightforward to obtain the autocorrelation $\phi_{r_I r_I}(\tau)$ from (2.10) and (2.1) as follows:

$$\begin{aligned}\phi_{r_I r_I}(t) &= E\left[r_I(t)r_I(t+\tau)\right] \\ &= \frac{\Omega_p}{2} E\left[\cos 2\pi f_{D,n}\tau\right] \\ &= \frac{\Omega_p}{2} E\left[\cos\left(2\pi f_m \tau\cos\theta\right)\right]\end{aligned} \tag{2.15}$$

where

$$\frac{\Omega_p}{2} = E\left[x^2(t)\right] = E\left[r_I^2(t)\right] = E\left[r_Q^2(t)\right] = \frac{1}{2}\sum_{n=1}^{N} E\left[\alpha_n^2\right] \tag{2.16}$$

is the total power from all the multipath components.

Likewise, the crosscorrelation is $\phi_{r_I r_Q}(\tau)$ is

$$\begin{aligned}\phi_{r_I r_Q}(\tau) &\triangleq E\left[r_I(t) r_Q(t+\tau)\right] \\ &= \frac{\Omega_p}{2} E_\theta\left[\sin(2\pi f_m \tau \cos\theta)\right]\end{aligned} \tag{2.17}$$

Evaluation of the expectations in (2.15) and (2.17) requires that we specify the probability density function for the angle of incidence of the arriving place waves, p(θ). For macrocellular applications, it is reasonable to assume that the place waves arrive at the MS antenna from all directions in the (x, y) plane with equal probability, i.e., θ is uniformly distributed over [-π, π]. This model was first suggested by Clarke [8], and is commonly referred to as Clarke's two-dimensional **isotropic scattering** model. With isotropic scattering, the expectation in (2.15) becomes

$$\phi_{r_I r_I}(\tau) = \frac{\Omega_p}{2} \frac{1}{2\pi} \int_{-\pi}^{\pi} \cos(2\pi f_m \tau \cos\theta) d\theta \tag{2.18}$$

$$= \frac{\Omega_p}{2} \frac{1}{\pi} \int_{0}^{\pi} \cos(2\pi f_m \tau \cos\theta) d\theta \tag{2.19}$$

$$= \frac{\Omega_p}{2} J_o(2\pi f_m \tau) \tag{2.20}$$

where $J_0(x)$ is the zero-order Bessel function of the first kind. Likewise, (2.17) becomes

$$\begin{aligned}\phi_{r_I r_Q}(\tau) &= \frac{\Omega_p}{2} \frac{1}{2\pi} \int_{-\pi}^{\pi} \sin(2\pi f_c \tau \cos\theta) d\theta \\ &= 0\end{aligned} \tag{2.21}$$

The normalized autocorrelation $\phi_{r_I r_I}(\tau) \big/ \left(\Omega_p / 2\right)$ is plotted against the normalized time delay $f_m \tau$ in Figure 7.

The power spectral density (PSD) of $r_I(t)$ and $r_Q(t)$ is the Fourier transform of $\phi_{r_I r_I}(\tau)$ or $\phi_{r_Q r_Q}(\tau)$, i.e.,

$$\begin{aligned}S_{r_I r_I}(f) &= \mathcal{F}\left[\phi_{r_I r_I}(\tau)\right] \\ &= \begin{cases} \dfrac{\Omega_p}{4\pi f_m} \dfrac{1}{\sqrt{1-\left(f/f_m\right)^2}} & |f| \le f_m \\ 0 & \text{otherwise} \end{cases}\end{aligned} \tag{2.22}$$

The autocorrelation of the received complex low-pass signal $r(t) = r_I(t) + j\, r_Q(t)$ is

$$\begin{aligned}\phi_{rr}(t) &= \frac{1}{2} E\left[r^*(t) r(t+\tau)\right] \\ &= \phi_{r_I r_I}(t) + j\phi_{r_I r_Q}(t)\end{aligned} \tag{2.23}$$

From (2.12) we have

$$\phi_{xx}(\tau) = \mathrm{Re}\left[\phi_{rr}(\tau) e^{j2\pi f \tau}\right] \tag{2.24}$$

Since $\phi_{rr}(\tau) = \phi_{rr}^*(-\tau)$, it follows that the PSD of the band-pass waveform $x(t)$ is

$$S_{xx}(f) = \frac{1}{2}\left[S_{rr}(f - f_c) + S_{rr}(-f - f_c)\right] \tag{2.25}$$

With isotropic scattering $\phi_{r_I r_Q}(\tau) = 0$ so that

$$S_{xx}(f) = \frac{1}{2}\left[S_{r_I r_I}(f - f_c) + S_{r_I r_I}(-f - f_c)\right] \tag{2.26}$$

where $S_{r_I r_I}(f)$ is given by (2.22).

RECEIVED ENVELOPE AND PHASE DISTRIBUTION

Rayleigh Fading

When the composite received signal consists of a large number of plane waves, the received complex low-pass signal $r(t) = r_I(t) + j\, r_Q(t)$ can be modeled as a complex Gaussian process. In the absence of a LOS or specular component, $r_I(t)$ and $r_Q(t)$ have zero mean. By using a bivariate transformation, the received complex envelope $z(t) = |r(t)|$ has a Rayleigh distribution at any time t, i.e.,

$$p_z(x) = \frac{x}{\sigma^2}\exp\left\{-\frac{x^2}{\sigma^2}\right\} \tag{2.27}$$

For a Rayleigh distributed envelope, the average power is $E[z^2] = \Omega_p = 2\sigma^2$ so that

$$p_z(x) = \frac{2x}{\Omega_p}\exp\left\{-\frac{x^2}{\Omega_p}\right\} \qquad x \geq 0 \tag{2.28}$$

This type of fading is called **Rayleigh fading** and agrees very well with empirical observations for macrocellular applications. Rayleigh fading usually applied to scenario where there is no LOS path between the transmitter and receiver antennas. By using a transformation of random variables, the squared-envelope $z^2(t) = |r(t)|^2$ is exponentially distributed with density

$$p_{z^2}(x) = \frac{1}{\Omega_p}\exp\left\{-\frac{x}{\Omega_p}\right\} \tag{2.29}$$

Thus, a non-uni-directional multipath fading, also known as non-line-of-sight (NLOS) fading results in a Rayleigh distribution of the received signal envelope at the MS for the simple case of an unmodulated signal. The power spectral density of the received inphase and quadrature components is independent of the carrier frequency and is only a function of the maximum possible Doppler frequency, given by the velocity of the mobile and the wavelength of the carrier.

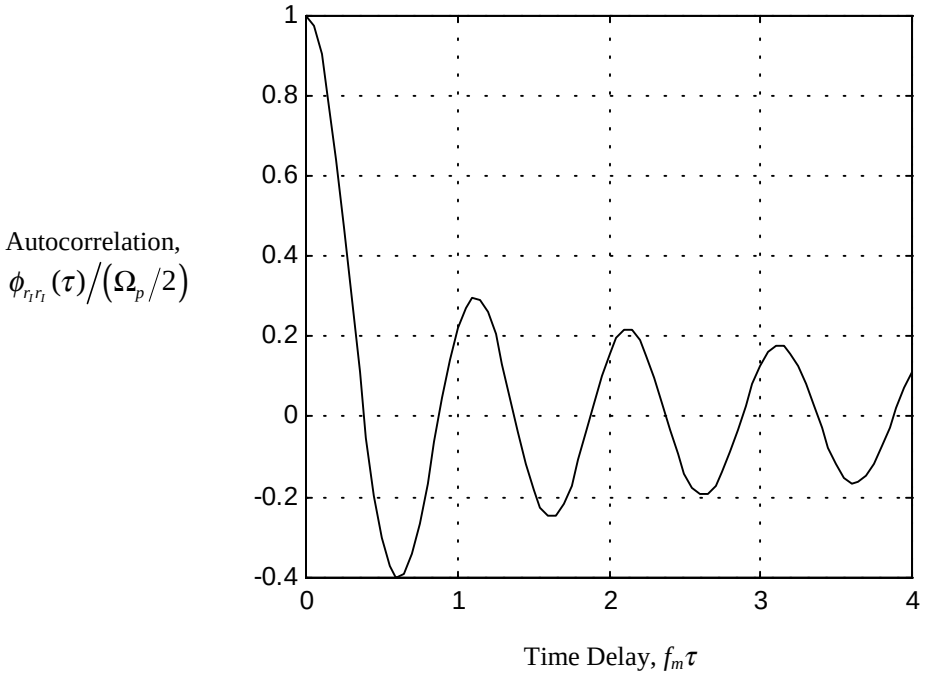

Figure 7 Autocorrelation of the inphase and quadrature components of the received complex low-pass signal for isotropic scattering

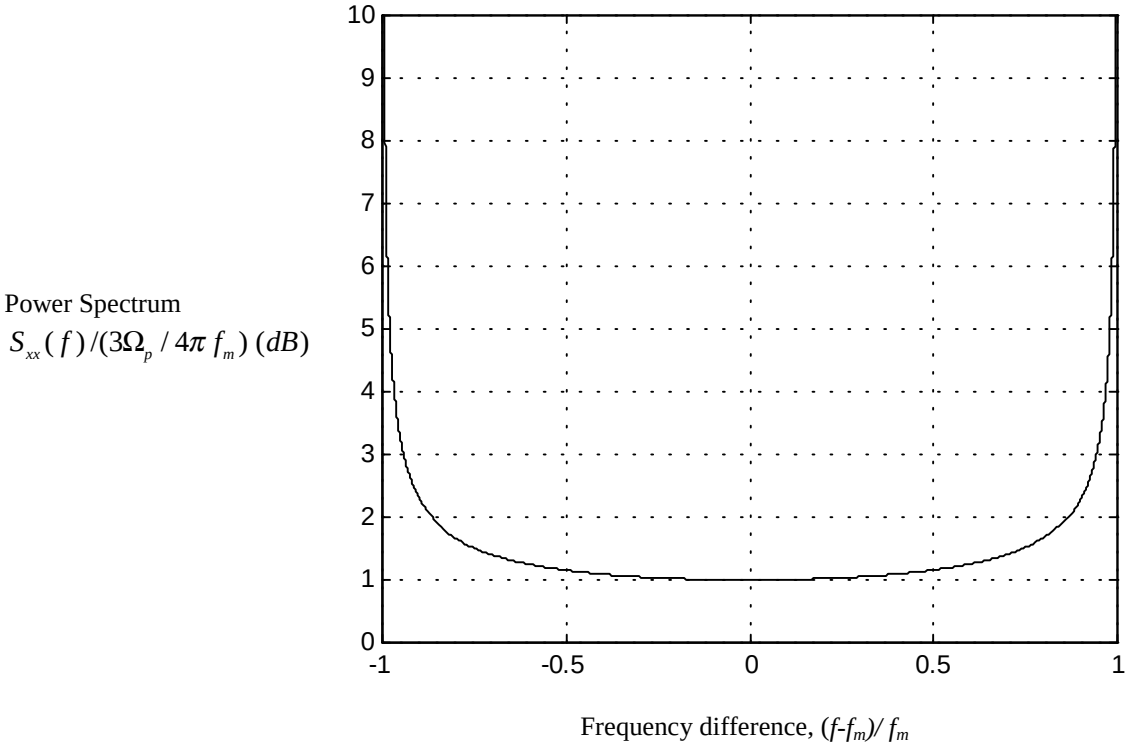

Figure 8 PSD of the received band-pass signal for an isotropic scattering channel

REFERENCES:

[1] Y. Omura, E. Ohmuri, T. Kawano, K. Fukuda, "Field strength and its variability in VHF and UHF land mobile radio service", *Rev. of the ECL*, Vol. 16, pp. 825-873, 1968.

[2] W. C. Y. Lee, *Mobile Communications Design Fundamentals*, Sams, Indianapolis, 1986.

[3] M. Hata and T. Nagatsu, "Mobile location using signal strength measurements in cellular systems," *IEEE Trans. on. Vehicular Technol*., Vol. 29, pp 245-352, 1980.

[4] COST 231 TD(91)109, "1800 MHz mobile net planning based on 900 MHz measurements", 1991.

[5] P. Harley, "Short distance attenuation measurements at 900 MHz and 1.8 GHz using low antenna heights for microcells," *IEEE Journal Selected. Areas of Communication*, Vol. 7, pp. 5-11, January 1989.

[6] O. Grimlund and B. Gudmundson, "Handoff strategies in microcellular systems," in *IEEE Vehicular Technology Conference*, Saint Louis, MO, pp. 505-510, May 1991.

[7] T. Rappaport, *Wireless Communications: Principles and Practice*, Prentice-Hall, NJ 1996.

[8] R. Clarke, "A statistical theory of mobile radio reception", *Bell System Technical Journal*, Vol. 47, pp. 957-1000, 1968.